Computers and Electronics in Agriculture 112 (2015) 2–9

Contents lists available at ScienceDirect

Computers and Electronics in Agriculture

journal homepage: www.elsevier.com/locate/compag

Sensing systems for precision agriculture in Florida

Won Suk Lee [a,*], Reza Ehsani [b,1]

[a] Agricultural and Biological Engineering Department, University of Florida, Gainesville, FL 32611, United States
[b] Citrus Research and Education Center, University of Florida, Lake Alfred, FL 33850, United States

ARTICLE INFO

Article history:
Received 1 June 2014
Received in revised form 8 October 2014
Accepted 3 November 2014
Available online 24 November 2014

Keywords:
Citrus
Disease
Machine vision
Mid-infrared
Near-infrared
Specialty crops

ABSTRACT

Many sensing systems have been developed for use in precision agriculture in Florida over the past decade. These systems have been designed for specialty crops such as citrus and blueberry. Systems include those for fruit recognition for yield mapping as well as those for disease detection systems using ground- and aerial-based platforms. Other systems discussed are used in soil phosphorus detection using near-infrared (NIR) and Raman spectroscopy, debris detection generated from citrus mechanical harvesting, detection of citrus fruit dropped on the ground due to disease, citrus leaf nitrogen detection, silage yield mapping, soil nutrients and grain insect detection using NIR spectroscopy. A summary of past efforts is presented in this paper, applications of these different sensing systems are discussed, and future directions are described.

1. Introduction

Precision technologies have been developed mostly for traditional crops since the advent of precision agriculture in the early 1990s. The concept of precision agriculture involves the assessment of in-field spatial variability of different factors such as fertility, soil type and characteristics, and water content in a field and the subsequent management of each crop production input in a more precise and site-specific manner according to the variability. However, in Florida, specialty crops such as citrus and blueberry are mainly grown, rather than traditional row crops, and therefore, alternative technologies are needed in order for precision agriculture to be applied. Over the past decade, much effort has been made to develop sensing technologies for site-specific crop management in Florida, and they were evaluated in actual crop production so that growers can increase yield and profit and maintain the quality of the environment to assure sustainability.

The United States is the second largest citrus producer in the world. Sixty-five percent of its citrus industry is in Florida, which corresponds to more than 450,000 acres of citrus groves. The Florida citrus industry has an estimated economic impact of $8.9 billion (Hodges and Spreen, 2012). In recent years, citrus production has been seriously affected by the emergence of exotic diseases such as citrus greening or Huanglongbing (HLB), citrus canker, and citrus black spot. Citrus production costs have increased from $800 per acre in 2004 to $1800 per acre in 2012. This $1000 increase in production cost in less than ten years is mainly due to additional costs of managing HLB disease. It has been estimated that citrus greening alone has cost about $3.63 billion in lost revenues. With globalization and expansion in the trade of agricultural commodities, this disease is feared to quickly spread from one area to another. Disease management is quickly become one of the most serious challenges in agriculture. In managing plant disease, detection is one of the most important steps. Detecting disease at an early stage, especially at the asymptomatic stage, could be the most cost-effective method of disease control. Currently, human scouting is most commonly used technique for disease detection in the majority of crops. However, human scouting is costly, time-consuming, and limited to human senses for the detection of disease. In recent years, progress in the area of low-cost, low-altitude satellites and unmanned aerial systems have provided an opportunity for continuous monitoring of plants. Such a crop monitoring system consists of a sensor system and a platform that carries the sensor. As shown in Fig. 1, the sensor could be hand-held, ground vehicle-based, or aerial-based. Changes in the spectral characteristics of the plant canopy in the visible, near-infrared (NIR), and mid-infrared (MIR) parts of electromagnetic spectrum are the basis for most commonly used sensors in detecting plant disease and stresses.

The objectives of this study are (1) to provide an overview of sensing systems for precision agriculture developed in Florida, which are different than those developed for traditional grain crops, and (2) to discuss and present future directions.

* Corresponding author. Tel.: +1 352 392 1864x207.
E-mail addresses: wslee@ufl.edu (W.S. Lee), ehsani@ufl.edu (R. Ehsani).
[1] Tel.: +1 863 956 8770.

http://dx.doi.org/10.1016/j.compag.2014.11.005
0168-1699/

2. Various sensing systems for fruit and tree crops

2.1. Fruit recognition

This section presents different sensing systems developed for identifying fruit and tree crops which are used in the development of fruit yield mapping systems. The yield mapping systems are considered as a first step in implementing precision agriculture.

2.1.1. Citrus yield mapping by detecting immature green and mature citrus

Various methods were developed to detect immature green and mature citrus fruit for the purpose of yield mapping. In the early 2000s, Annamalai and Lee (2003) developed an image processing algorithm to detect citrus fruit in an image using hue and saturation thresholds of citrus fruit, leaves, and background classes. They reported an R^2 of 0.76 between the number of fruit by the machine vision algorithm and the number by manual counting. The total processing time for an image was 283 ms with a 750 MHz Pentium processor excluding image acquisition time. Further, Annamalai and Lee (2004) investigated spectral signatures of immature green citrus fruit and leaves for the purpose of developing spectral-based fruit identification and an early yield mapping system. Diffuse reflectance of fruit and leaf samples were measured in the range of 400–2500 nm, and two important wavelengths, 815 nm and 1190 nm, were identified as shown in Fig. 2. A ratio of these two wavelengths was used to distinguish immature green fruit from leaves.

Zaman and Schumann (2005) utilized an ultrasonic system to measure citrus tree volumes in Florida and compared the results with manual measurements. They also investigated relationships between tree volumes measurements and row spacings as well between tree volumes and tree ages. Their measurements produced good results with manual measurements (R^2 = 0.95–0.99). They found out that the ultrasonic measurements were more accurate for young trees with narrower row spacing and that more frequent measurements would be needed for groves with wider spacing and old trees. Further Zaman et al. (2006) extended the ultrasonic measurement of tree volumes to fruit yield estimation. Their results from a 17 ha Valencia grove in Florida yielded an average fruit yield prediction accuracy of 90.6% with a root mean square error (RMSE) of 4.2 Mg/ha. They reported that the relationship between ultrasonic tree size and fruit yield was significant with an R^2 of 0.80. In another citrus fruit recognition study, Bulanon et al. (2009) implemented image fusion of a visible image and a thermal infrared image to increase fruit identification. They performed image registration, Laplacian pyramid transform, and

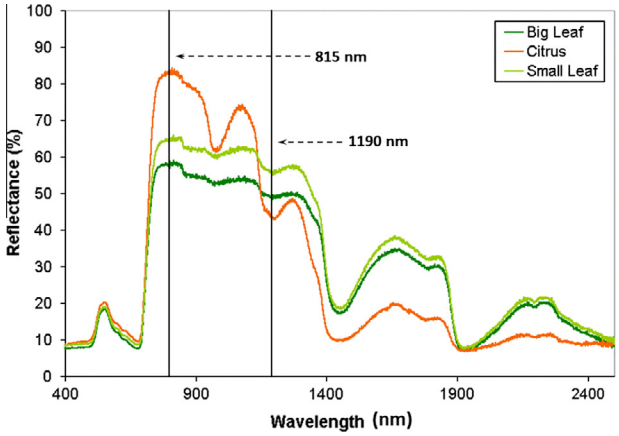

Fig. 2. Reflectance spectra of immature green citrus and leaves (adapted from Annamalai and Lee (2004)).

fuzzy logic to detect fruit and reported that fuzzy logic was better for identifying fruit due to its robust inference engine.

Employing an outdoor hyperspectral imaging system, Okamoto and Lee (2009) developed algorithms to detect green immature citrus for three different varieties using the range of 369–1042 nm. A linear discriminant analysis for pixels was used to identify fruit objects and spatial image processing steps were used to detect green citrus. They reported detection accuracies of 70–85% depending on citrus varieties and 80–89% accuracy for the fruit in the foreground. For a combined set of three varieties, a 75.8% success rate was reported for the validation set images. Young leaves were the main obstacle for correction identification since they were spectrally very similar to green citrus.

Since hyperspectral imaging systems are usually expensive, attempts were made to utilize a typical consumer-grade digital camera to detect immature green citrus fruit. Kurtulmus et al. (2011) developed a machine vision algorithm to distinguish immature green citrus fruit from other objects in natural outdoor color digital images using color, circular Gabor texture, and a novel 'eigenfruit' method. They reported a correct identification of 75.3% for immature green citrus for a validation set. In Bansal et al. (2013), a percent leakage of the fast Fourier transform was used to distinguish fruit from other objects in natural outdoor color digital images, and 82% of fruit were correctly identified from a set of 60 validation images. Also, Sengupta and Lee (2014) developed a method for identifying immature green citrus from digital color images and reported a detection accuracy of 80.4% in a validation set. A Hough circle detection and texture classification by a support vector machine (SVM) were used to find all potential citrus fruit.

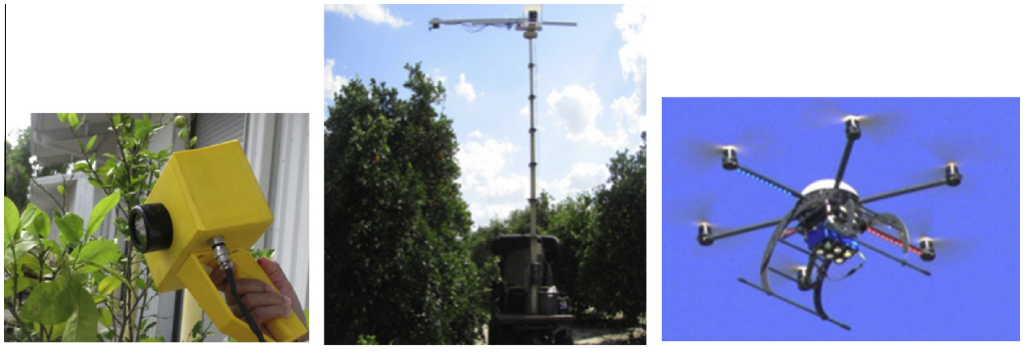

(a) (b) (c)

Fig. 1. Types of sensor on a crop monitoring system: (a) hand-held, (b) ground vehicle-based, and (c) aerial-based.

Then, false positives were removed using Canny edge detection and keypoints obtained by a scale invariant feature transform (SIFT). They reported that varying illumination, partial occlusion in outdoor images, and detecting immature green citrus in the presence of green leaves were major problems and that an additional method would be needed to remove more false positives.

2.1.2. Determining citrus count and size on a citrus mechanical harvester and debris cleaning machine

A study was conducted to develop a yield mapping system for a citrus mechanical harvester. Chinchuluun et al. (2009) developed a machine-vision based citrus fruit counting system for a continuous canopy shake and catch harvester. A Bayesian classifier along with morphological operations and a watershed algorithm was used. The algorithm was able to identify the mass of citrus fruit successfully with an R^2 of 0.96 between the actual and estimated fruit mass when the classifier was evaluated on a test bench. The number of fruit was also estimated using a Bayesian classifier with an R^2 of 0.89.

Due to infectious citrus diseases such as citrus black spot, growers are required to dispose of leaves and twigs in the grove before transporting harvested fruit to juice processing plants or cover their load with tarp to avoid spread of infected plant materials. Patil et al. (2009) developed a system for removing debris and quantifying its mass from a continuous canopy shake and catch harvester for citrus using a machine vision and a set of pinch rollers. They reported that mass estimation of debris materials yielded an R^2 of 0.84 using pixel areas in the images. They also reported problems of large twigs stopping rotation of rollers due to being trapped in between rollers and varying sunlight intensity in acquiring high quality images. In order to estimate mass of debris generated from mechanical harvesting, Bansal et al. (2011) developed a machine vision system using various image processing steps and a novel "Parse and Add" algorithm. They achieved an R^2 of 0.946 between actual and estimated debris mass and an R^2 of 0.815 between the actual and the estimated debris mass with an RMSE of 1.88 kg. They also generated a map of the debris mass from a field experiment as shown in Fig. 3. This map could be used to identify important factors related to debris generation and to efficiently manage trees to reduce the amount of debris in future harvesting.

For a debris cleaning system as shown in Fig. 4, Shin et al. (2012) developed an in-field machine vision system capable of estimating citrus fruit count, fruit mass, and fruit size. Pixel classification algorithms using logistic regression were developed and a highly saturated area recovering (HSAR) algorithm was implemented to reduce any incorrect identification of fruit due to the highly saturated area on fruit surface. They reported a coefficient of determination of 0.945 between the measured fruit mass and the estimated fruit mass with a RMSE of 116 kg. A watershed algorithm with an H-minima transform was implemented for a more accurate fruit count and recognition.

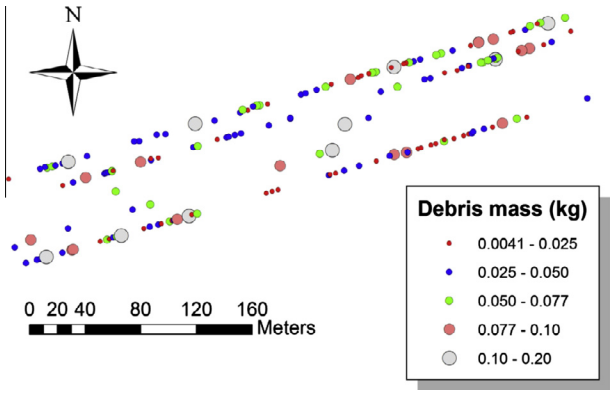

Fig. 3. A geo-referenced map of debris mass estimated from images (adapted from Bansal et al. (2011)).

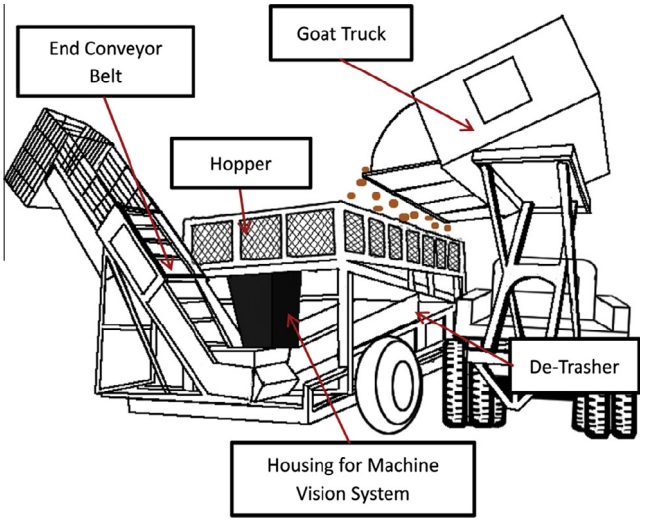

Fig. 4. In-field debris cleaning machine for mechanically harvested citrus (adapted from Shin et al. (2012)).

2.1.3. Other fruit detection systems

As a first step toward the development of a blueberry yield mapping system, Yang et al. (2012) investigated spectral signatures of seven representative southern highbush blueberry varieties for the development of a blueberry yield mapping system. Reflectance of blueberry fruit samples at different growth stages (mature, near-mature, near-young, young, and leaf) was measured in the range of 200–2500 nm, and normalized indices were used to classify them. Classification tree, principal component analysis and multinomial logistic regression techniques were used to identify fruit growth stages, and accuracies of 95–100% were obtained for fruit and leaf classification. Important wavelengths were identified for fruit recognition, which can be used for yield mapping using multispectral imaging. In another study, Kurtulmus et al. (2014) developed machine vision algorithms for immature peach fruit detection on trees that can be used to create yield maps and to adjust management practices to increase yield and profit. Regular digital color images of peach tree canopies were acquired under natural illumination conditions and used for fruit identification using circular Gabor texture, an 'eigenfruit' approach, statistical classifiers, a neural network, and a support vector machine. Correct detection accuracies of 71–84% were obtained depending on image scanning methods used.

2.2. Disease detection systems for citrus

This section compares the results and studies of different optical techniques used in detecting citrus HLB and citrus canker diseases. This section presents the advantages and disadvantages of different techniques and their applications in disease detection. Table 1 summarizes various methods for detecting citrus diseases and stress.

2.2.1. Visible and NIR bands

Visible and NIR bands are ideal for developing sensors for disease detection because the detectors used in this part of the

electromagnetic spectrum are relatively inexpensive. The first step in developing a sensor for detecting a specific disease is to find a specific spectral signature associated with that particular disease. This part is usually done with a portable spectrometer, and data are collected in the 350–2500 nm range.

Sankaran and Ehsani (2013) used a portable spectrometer (SVC HR-1024) in the 350–2500 nm range for detection and classification of citrus greening or HLB and citrus canker from healthy trees. They used quadratic discriminant analysis and a K-nearest neighbor classifier; both techniques provided a high percent of detection accuracy. Similar studies were performed with different classification techniques by Sankaran and Ehsani (2011), Mishra et al. (2012), and Sankaran et al. (2013). Sankaran et al. (2012) also used a hand-held spectrometer to collect data from asymptomatic, symptomatic, freeze-damaged, and healthy plants. Linear discriminant analysis, quadratic discriminant analysis, Naïve-Bayes, and bagged decision trees were used as classifiers with 77%, 92%, 84%, and 99% accuracy, respectively. All classifiers were able to discriminate symptomatic-infected leaves from freeze-damaged leaves, but some asymptomatic leaves were incorrectly detected as a healthy leaves.

Low-cost, rugged disease specific sensors can be built by using only a few selected bands rather than collecting the spectral data in the whole range of visible and NIR bands. Multi-band sensors are high density illuminators at a specific narrow band for detecting disease and stress. These bands are either tailored for a specific disease or they use two bands in the red and NIR range to calculate the normalized difference vegetation index for general stress detection. Mishra et al. (2011) used a four-band active optical sensor for detecting HLB in citrus, two of which were in the visible region (570 and 670 nm), whereas the other two were in the NIR region (750 nm and 870 nm). They used the K-nearest neighbor, support vector machines, and the decision tree as classification techniques and achieved 96%, 97%, and 95.5% accuracy, respectively.

Table 1
Various methods for detecting citrus diseases and stress.

Method	Fruit disease	Category of trees	Device	Range	Classifier	Accuracy (%)
Airborne multispectral	HLB	HLB1 HLB2 Nutrient deficient Healthy	SVC HR-1024	Blue (430–470 nm) Green (530–570 nm) Red (630–670 nm) NIR (810–850 nm)	SAM MTMF LSU	(SAM) 80–86.6
Airborne hyperspectral	HLB	HLB1 HLB2 Nutrient deficient Healthy	SVC HR-1024	128 bands (457.2–921.7 nm with 3.63 intervals)	SAM MTMF LSU ESAM	60–66.6 73.3–80 56.6–73.3 86
Airborne hyperspectral	HLB	Diseased Healthy	AISA EAGLE VNIR	Blue (450–510 nm) Green (510–580 nm) Red (630–690 nm) NIR (770–895) Coastal (400–450 nm) Yellow (585–625 nm) Red-edge (705–745 nm) Longer NIR (860–1040 nm)	ESAM	86
Visible-NIR	HLB and canker	Diseased Healthy	SVC HR-1024	350–2500 nm	QDA KNN SIMCA LDA	92.5 ± 5.3 89.4 ± 7 91.7 90.3
Visible-NIR	HLB	Diseased Healthy	ASD	350–2500 nm	KNN SVM LR	93.5 97 81
Visible-NIR	HLB	Diseased Healthy	MCA, MIC-005	440–900 nm	LDA QDA BDT SVM	81 ± 6 80 ± 6 80 ± 3 87 ± 3
Visible-NIR (using vegetation indices)	HLB	Diseased Healthy	SVC HR-1024	350–2500 nm	GDA SIMCA	80–83 68–84
MIR	HLB & canker	Diseased Healthy	InfraSpec VFA-IR	5.15–10.72 μm	QDA KNN	98 ± 0.9 99 ± 0.9
Fluorescence spectroscopy	HLB	Diseased Nutrient deficient Healthy	Multiplex 3	UV Blue Green Red	NB BDT	85 >94
Active optical sensor	HLB	Diseased Healthy	Active optical sensor	Visible (570, 670 nm) NIR (870, 970 nm)	KNN SVM BDT	96 97 95.5
Hyperspectral radiometry	HLB	Diseased Healthy	SVC HR-1024	350–2500 nm	LR	>90
Thermal imaging	HLB	Water Stress	TAU 640	7.5–13.5 μm	NB BDT	80
MIR	HLB	Diseased Nutrient deficient Healthy	InfraSpec VFA-IR	5.15–10.72 μm	KNN QDA	98.8 80

2.2.2. Mid-infrared bands

MIR refers to the radiation band in the range of 2500–50,000 nm. MIR spectroscopy usually requires sample preparation which is a disadvantage compared to NIR spectroscopy. However, MIR spectroscopy has some advantages over NIR spectroscopy. One of the major advantages of MIR spectroscopy is that many chemicals have a fundamental peak or signature in this region which makes spectral interpretation easy compared to the NIR region where the spectra is composed of overlapping overtones of absorption bands of many interfering chemicals. Sankaran and Ehsani (2013) used a portable MIR spectrometer (InfraSpec VFA-IR) in the range of 5.15–10.72 μm to detect healthy leaves as well as those infected with HLB and canker. The leaves were ground into a fine powder and were placed on the crystal window of a MIR spectrometer. The scan time was 1 min. Quadratic discriminant analysis and K-nearest neighbor were used as classifiers, and resulted in high accuracies of 98 ± 0.9% and 99 ± 0.9%, respectively.

2.2.3. Fluorescence spectroscopy

Fluorescence spectroscopy is another optical sensing technique that is widely used for plant stress detection. A hand-held multi-parameter optical sensor (Multiplex® 3) was used to detect HLB disease in leaves of two different sweet orange cultivars, Hamlin and Valencia. This sensor is a non-destructive real-time sensor. Four excitation wavelengths were used: UV, blue, green, and red. For each wavelength, yellow, red, and far-red fluorescence was measured. The classifiers used were Naïve-Bayes and bagged decision tree with accuracies of 85% and greater than 94%, respectively. The bagged decision tree classifier had a better performance in comparison with Naïve-Bayes; however, it needed more time for the computation process, at least 10 times more than the Naïve-Bayes (Sankaran and Ehsani, 2012).

2.2.4. HLB detection using polarized light

The HLB-symptomatic citrus leaves exhibit starch accumulation, which in turn resulted in rotating the polarization planar of light near 600 nm. Pourreza et al. (2014) developed a detection system for HLB disease using narrow-band imaging and polarized filters. Four groups of textural features and seven classifiers were used to detect HLB-symptomatic leaves, and accuracies of 93.1% and 89.6% were reported for Hamlin and Valencia varieties, respectively.

2.2.5. HLB detection by airborne hyperspectral and multispectral imaging

Aerial hyperspectral imaging can rapidly detect potentially disease-infected trees within a large area and can be very useful for quickly identifying areas where inspections should be focused, since ground inspection is time consuming and labor intensive. Kumar et al. (2012) utilized two sets of aerial hyperspectral and multispectral images for the HLB detection. An image-derived spectral library, spectral angle mapping (SAM), mixture tuned matched filtering (MTMF), and linear spectral unmixing were used. They obtained a detection accuracy of 87% using multispectral images and an accuracy of 80% for one of the test sites using hyperspectral images. One of the main sources of error was sample coordinates due to possible inaccurate ground truthing. MTMF yielded a better result than SAM. Different vegetation indices such as anthocyanin reflectance index (ARI), atmospheric resistant vegetation index (ARVI), carotenoid reflectance index (CRI), and red edge normalized difference vegetation index (RENDVI) were used to remove false positives. Li et al. (2012) also acquired aerial hyperspectral and multispectral images to detect HLB disease, analyzed spectral features of healthy and symptomatic canopies, and achieved various levels of accuracies (28–90% for hyperspectral images and 59–95% for multispectral images) using different classification methods including parallelepiped, minimum distance, Mahalanobis distance, SAM, spectral information divergence (SID), spectral feature fitting (SFF), and MTMF. They reported that a simple red edge position (REP) worked well with a 90% accuracy to identify HLB-infected canopy from ground measurements; however, it did not work for the aerial images due to low spatial resolution. Further, Li et al. (2014) proposed a novel method, 'extended SAM (ESAM)', for the purpose of developing a standard procedure to detect HLB-infected canopies in aerial hyperspectral images. The ESAM method consisted of noise removal using the Savitzky-Golay smoothing, background pixel removal using SVM, pure endmember selection using vertex component analysis (VCA), detection of infected canopy by SAM, and false positive removal using REP. When compared with the traditional SAM, they described that VCA and REP were the main advantages since VCA could select pure endmembers, and REP could remove false positives by utilizing the unique vegetation characteristics. The ESAM method yielded detection accuracies of 64–86% for HLB-infected trees, while both Mahalanobis distance and K-means yielded an accuracy of 64% using the same dataset.

2.2.6. Identification of other citrus diseases

Another study was conducted to identify other citrus diseases. Pydipati et al. (2006) investigated the potential of using the color co-occurrence method (CCM) to detect normal and diseased (greasy spot, melanose, and scab) citrus leaves in a laboratory. Discriminant analysis using CCM textural features obtained from hue, saturation, and intensity (HSI) yielded correct identification of more than 95% for all diseases. They reported that data models using hue and saturation features produced higher detection accuracies when compared with models developed using intensity, indicating that they can be better used under varying light conditions.

2.3. Other sensing systems

2.3.1. Soil phosphorus detection using NIR and Raman spectroscopy

In Florida, excess phosphorus (P) entering from agricultural fields, dairy farming, and beef cattle ranching in Lake Okeechobee causes many problems such as periodic algal blooms and displacement of native ecosystems. Typically P concentration is measured from the samples obtained at monitoring stations in the lake through standard laboratory analysis procedure, which is very time consuming, costly and labor intensive. Thus, to facilitate the identification of problem areas ("hot-spots") throughout the drainage basin, various techniques were investigated for cost-effective P detection which can decrease the time and labor required for monitoring P-levels in the Lake Okeechobee region. Bogrekci and Lee (2005a) used ultraviolet (UV), visible, and NIR spectroscopy in 225–2550 nm to determine soil and grass P concentrations. Absorbance spectra of dry soil and vegetation are shown in Fig. 5. Stepwise multiple linear regression (SMLR) and partial least squares (PLS) analyses were used to develop prediction models. Strong predictions were obtained for soil P concentrations with R^2 of 0.922, 0.914, and 0.778 for total P, Melich-1 P, and water-soluble P, respectively, however the models did not work well for grass P concentrations (R^2 = 0.435).

Also Bogrekci and Lee (2005b) studied the effect of soil particle size on application of the reflectance spectroscopy to determine P concentrations. Fig. 6 shows absorbance of wet and dry sandy soil samples with different particle sizes. They reported that coarse soil particles absorbed more light than medium and fine particles. Using multiple linear regression and linear partial least squares,

soil P concentrations were estimated better if soil particle sizes of unknown samples were identified first.

In order to identify soil spectral signatures for the purpose of determining their P concentrations, Bogrekci and Lee (2005c) collected a total of 345 soil samples in 10 different locations in the Lake Okeechobee drainage basin in Florida and measured reflectance in the UV–VIS–NIR regions. The soil samples in a calibration set were leached and subtracted from those in the validation set to obtain only the spectrum of soil constituents. PLS prediction models yielded R^2 values of 0.83 and 0.97 for the original soil and constituent spectra, respectively. In another study, Bogrekci and Lee (2005d) identified spectral signatures of four commonly-found phosphates ($CaPO_4$, $AlPO_4$, $FePO_4H_2O$, and $Mg_3(PO_4)H_2O$) in the Lake Okeechobee drainage basin in Florida. Fig. 7 illustrates absorbance spectra of the four soil phosphates in Florida. Important wavelengths were identified using stepwise discriminant analysis to build prediction models for P concentrations. They reported that different P compounds could be identified with 1.9% classification error, and P concentrations were able to be estimated with an R^2 of 0.48–0.75 and an RMSE ranging from 27 to 43 mg/kg.

In order to reduce prediction errors obtained from the NIR system (Bogrekci and Lee, 2005a), Raman spectroscopy was adopted to develop a portable field sensor system (Fig. 8), which consisted of a laser source at 785 nm, a laser probe assembly, a spectrometer, and a computer (Bogrekci and Lee, 2005e). They used PLS and SMLR to analyze Raman spectra of soil samples and reported an R^2 of 0.98 and an RMSE of 151 mg/kg using a PLS prediction model for P concentrations. Further, Bogrekci and Lee (2006) investigated the effect of soil particle size in Raman spectroscopy to enhance accuracy of soil P estimation. They found that P concentration could be estimated better when the sample contains similar particle sizes, and suggested grinding soil samples to make them uniform size before spectral measurement.

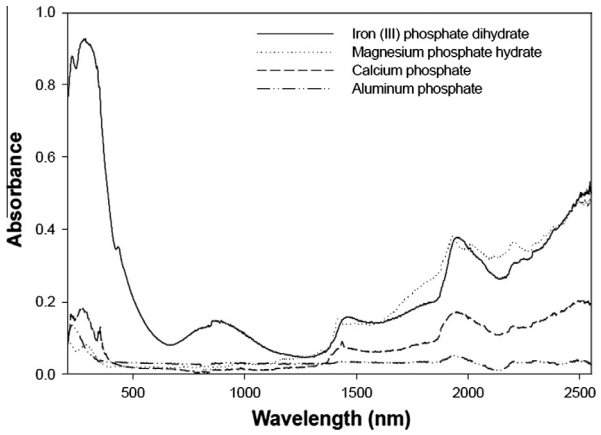

Fig. 7. Average absorbance of four common soil phosphates (adapted from Bogrekci and Lee (2005d)).

2.3.2. Detection of citrus dropped on the ground

In recent years, premature citrus fruit drop before harvesting has become a major problem in Florida. It would be very difficult to manually count dropped fruit, and an automated system would be needed. Choi et al. (2013) developed a machine vision system to estimate the number of fruit prematurely dropped on the ground before being harvested, mainly due to HLB and unfavorable environmental conditions. Along with a DGPS receiver, two rugged outdoor cameras equipped with a microprocessor were installed on the front of a truck and were used for imaging. They implemented the Retinex algorithm to enhance the illumination of images, and different classifiers (logistic regression, KNN and Bayesian) were used to detect fruit which yielded accuracies of 88%, 84%, and 83%, respectively. A georeferenced fruit drop map was created to help growers manage the problem more efficiently.

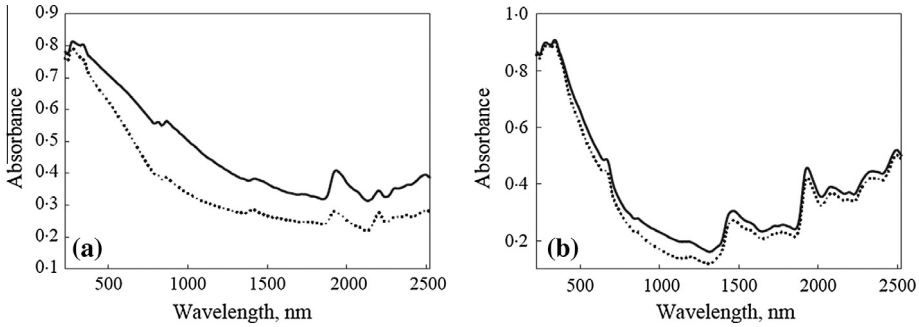

Fig. 5. Absorbance spectra of (a) dry soil and (b) dry vegetation samples with high (solid line) and low (dotted line) P concentrations (adapted from Bogrekci and Lee (2005a)).

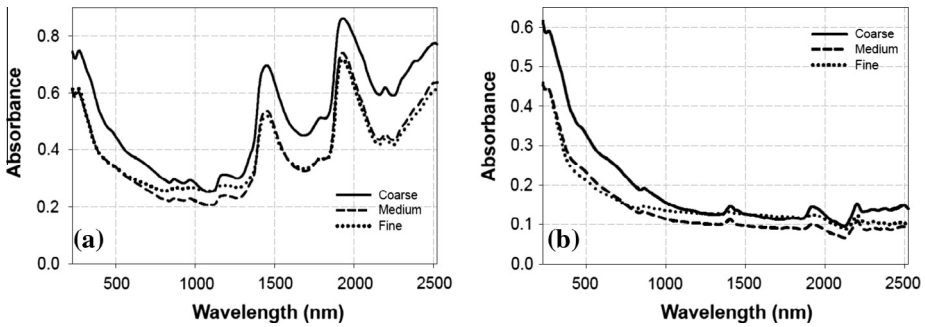

Fig. 6. Absorbance spectra of (a) wet sandy soil (8%) and (b) dry sandy soil samples with three particle sizes without any P concentration (adapted from Bogrekci and Lee (2005b)).

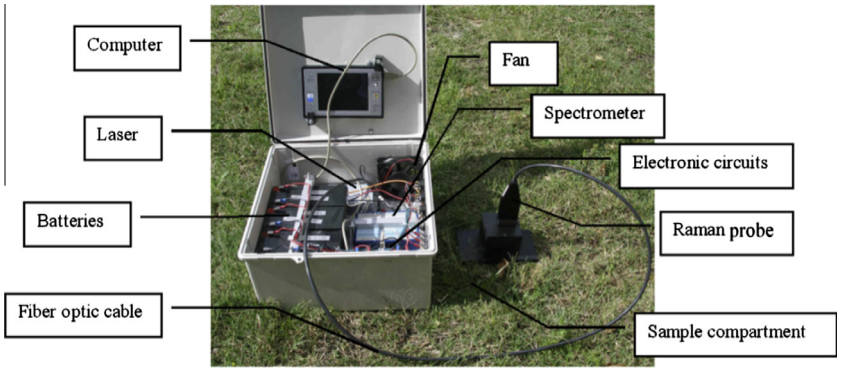

Fig. 8. A prototype portable Raman P sensor (adapted from (Bogrekci and Lee, 2005e)).

2.3.3. Nitrogen detection in citrus leaves and Chinese cabbage

Min and Lee (2005) investigated significant wavelengths for detection of nitrogen content in citrus leaves using NIR spectroscopy and multivariate statistical analyses. Fig. 9 illustrates absorbance spectra of citrus leaves with two different nitrogen concentrations. They identified 448, 669, 719, 1377, 1773, and 2231 nm as important wavelengths using a SMLR and a PLS regression. The best prediction model by SMLR yielded an R^2 of 0.839 with an RMSD of 0.122% of nitrogen concentration. Further, Min et al. (2006) extended the investigation to detect the nitrogen (N) content of Chinese cabbage seedlings using VIS–NIR spectroscopy. A wavelength of 710 nm was identified as the most important wavelength for estimating N content, and some water-related wavelengths of 1467, 1910, and 1938 nm were found to be important in estimating N content.

2.3.4. Silage yield mapping system

Lee et al. (2005) developed a silage yield mapping system that consisted of a DGPS receiver, load cells, a header switch, Bluetooth modules for wireless transmission of moisture data, and a moisture sensor. The system was tested in commercial silage fields, and yielded errors in estimating silage mass between −1.95% and 4.9%, compared to mass measured by a platform scale. An example silage yield map is shown in Fig. 10.

2.3.5. Grain insect detection using NIR

Using NIR spectroscopy, Khedher Agha et al. (2013) developed prediction models for degrees of insect infestation (DI) in triticale seeds. Reflectance was measured in the range of 400–2500 nm for seed samples infested with 11 different DIs of two life cycle stages of the insect (larvae 2nd instar and adult outside seed). Prediction modes developed by SMLR yielded an R^2 of 0.87 for both the larvae and insect outside stages. They reported that prediction of the early growth stage was more difficult than the adult stage since the insect size at the instar stage was smaller.

3. Summary and conclusions

This study reviewed various sensing systems developed for precision agriculture in Florida. In Florida, more specialty crops are grown than grain crops for which precision technologies were originally developed. In this study, sensing systems are described including a yield mapping system that uses fruit recognition, disease detection sensors that are carried by ground- and aerial-based platforms, soil P detectors that use NIR and Raman spectroscopy, debris detectors for mechanically harvested citrus, an N detector for citrus leaves, a silage yield mapping system, and soil nutrient and grain insect detectors using NIR spectroscopy.

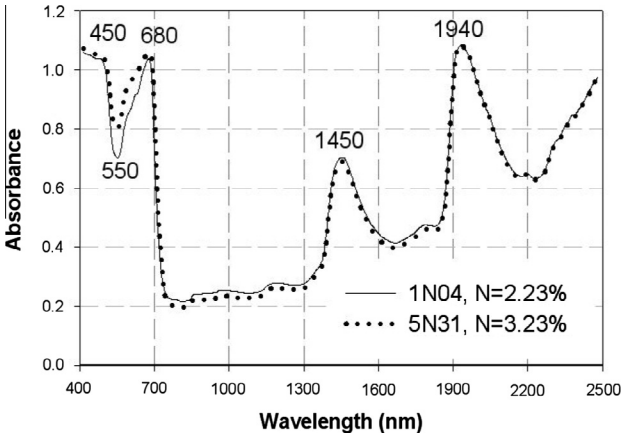

Fig. 9. Example of absorbance spectra of citrus leaves with two different amounts of N content (adapted from Min and Lee (2005)).

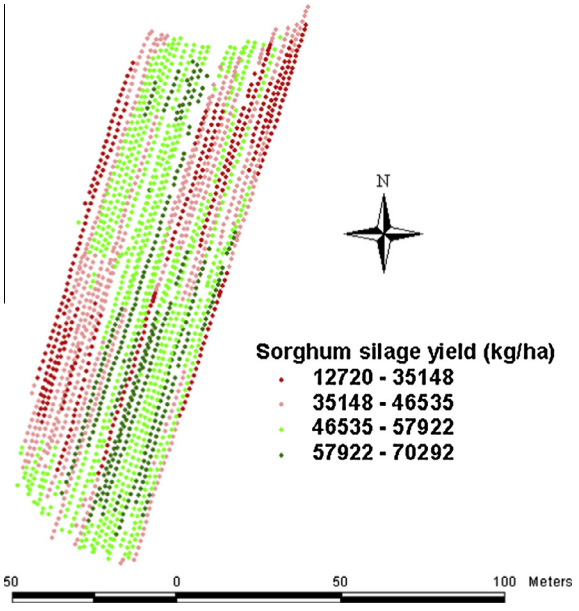

Fig. 10. Sorghum silage yield map (adapted from Lee et al. (2005)).

Applications of visible, NIR, and MIR spectroscopy and imaging for disease detection have also been reviewed. In general, developing a disease detection system at the symptomatic stage is relatively easier than at the asymptomatic stage. However, in most

cases, disease detection systems are more useful if they can detect the disease at the asymptomatic stage where human scouts are not capable of detecting the disease.

4. Future recommendations

Florida's agriculture is dominated by specialty crops such as sugarcane, citrus, strawberry and tomato. This unique type of production system requires more creative and adaptive technologies that are not commonly available. Among the sensing systems developed, the following have great potential to be adopted by the growers: immature green citrus detection, debris detection and cleaning system (currently in the process of being patented), blueberry yield mapping system, the HLB detection systems developed using optical properties and starch accumulation, silage yield mapping, grain insect detection using NIR, soil P sensing systems, citrus debris detection system from mechanical harvesting, and detection of dropped citrus fruit on the ground.

However, since the market for specialty crops is relatively small, many manufacturers of sensors and sensing technology cannot justify the research and development costs to develop new sensing systems for specialty crops as this would take a long time and require much effort.

Before developing sensing systems, it is important to understand the needs of the growers. For example, sensing systems for irrigation and primary nutrients such as N, P, and potassium could be high priorities for growers.

Growers are inclined to adopt new technology that is cost effective and has a high return on investment. Most importantly, it should be based on credible science. The availability of inexpensive, reliable, durable, user-friendly, and rugged sensing systems are important for future adoption of precision technologies. New technologies such as unmanned aerial vehicles enable growers to more efficiently utilize sensors in their field operations.

Acknowledgements

The authors would like to thank and acknowledge the contributions that were made by all students, postdocs, technicians, faculty members, visiting scholars, and growers as well as agencies who funded the projects that were described in this article over the past decade.

References

Annamalai, P., Lee, W.S., 2003. Citrus yield mapping system using machine vision. ASAE Paper No. 031002. St. Joseph, Mich., ASAE.

Annamalai, P., Lee, W.S., 2004. Identification of green citrus fruits using spectral characteristics. ASAE Paper No. FL04-1001. St. Joseph, Mich., ASAE.

Bansal, R., Lee, W.S., Satish, S., 2013. Green citrus detection using fast fourier transform (FFT) leakage. Precis. Agric. 14 (1), 59–70. http://dx.doi.org/10.1007/s11119-012-9292-3.

Bansal, R., Lee, W.S., Shankar, R., Ehsani, R., 2011. Automated debris mass estimation for citrus mechanical harvesting systems using machine vision. Appl. Eng. Agric. 27 (5), 673–685.

Bogrekci, I., Lee, W.S., 2005a. Spectral phosphorus mapping using diffuse reflectance of soils and grass. Biosyst. Eng. 91 (3), 305–312.

Bogrekci, I., Lee, W.S., 2005b. Improving phosphorus sensing by eliminating soil particle size effect in spectral measurement. Trans. ASAE 48 (5), 1971–1978.

Bogrekci, I., Lee, W.S., 2005c. Spectral soil signatures and sensing phosphorus. Biosyst. Eng. 92 (4), 527–533.

Bogrekci, I., Lee, W.S., 2005d. Spectral measurement of common soil phosphates. Trans. ASAE 48 (6), 2371–2378.

Bogrekci, I., Lee, W.S., 2005e. A Raman sensor for phosphorus sensing in soil and vegetations. ASAE Paper No. 051040. St. Joseph, Mich., ASAE.

Bogrekci, I., Lee, W.S., 2006. The effect of particle size on sensing phosphorus by Raman spectroscopy. ASABE Paper No. 063048. St. Joseph, Mich., ASABE.

Bulanon, D.M., Burks, T.F., Alchanatis, V., 2009. Image fusion of visible and thermal images for fruit detection. Biosyst. Eng. 103 (1), 12–22.

Chinchuluun, R., Lee, W.S., Ehsani, R., 2009. Machine vision system for determining citrus count and size on a citrus canopy shake and catch harvester. Appl. Eng. Agric. 25 (4), 451–458.

Choi, D., Lee, W.S., Ehsani, R., Banerjee, A., 2013. Detecting and counting citrus fruit on the ground using machine vision. ASABE Paper No. 131591603. St. Joseph, Mich., ASABE.

Hodges, A.W., Spreen, T.H., 2012. Economic impacts of citrus greening (HLB) in Florida. EDIS document FE903. Food and Resource Economics Department, Florida Cooperative Extension Service, Institute of Food and Agricultural Sciences, University of Florida, Gainesville, FL.

Khedher Agha, M.K., Lee, W.S., Wang, C., Mankin, R.W., Bliznyuk, N., Bucklin, R.A., 2013. Determination degrees of insect infestation in triticale seed using NIR spectroscopy. ASABE Paper No. 131592957. St. Joseph, Mich., ASABE.

Kumar, A., Lee, W.S., Ehsani, R., Albrigo, L.G., Yang, C., Mangan, R.L., 2012. Citrus greening disease detection using aerial hyperspectral and multispectral imaging techniques. J. Appl. Remote Sens. 6, 063542, http://link.aip.org/link/doi/10.1117/1.JRS.6.063542.

Kurtulmus, F., Lee, W.S., Vardar, A., 2011. Green citrus detection using eigenfruit, color and circular Gabor texture features under natural outdoor conditions. Comput. Electron. Agric. 78 (2), 140–149.

Kurtulmus, F., Lee, W.S., Vardar, A., 2014. Immature peach detection in colour images acquired in natural illumination conditions using statistical classifiers and neural network. Precis. Agric. 15, 57–79. http://dx.doi.org/10.1007/s11119-013-9323-8.

Lee, W.S., Schueller, J.K., Burks, T.F., 2005. Wagon-based silage yield mapping system. Agric. Eng. Int.: CIGR J., vol. VII. Manuscript IT 05 003. cigr-ejournal.tamu.edu.

Li, H., Lee, W.S., Wang, K., Ehsani, R., Yang, C., 2014. 'Extended spectral angle mapping (ESAM)' for citrus greening disease detection using airborne hyperspectral imaging. Precis. Agric. 15, 162–183. http://dx.doi.org/10.1007/s11119-013-9325-6.

Li, X., Lee, W.S., Li, M., Ehsani, R., Mishra, A., Yang, C., Mangan, R.L., 2012. Spectral difference analysis and airborne imaging classification for citrus greening infected trees. Comput. Electron. Agric. 83, 32–46.

Min, M., Lee, W.S., 2005. Determination of significant wavelengths and prediction of nitrogen content for citrus. Trans. ASAE 48 (2), 455–461.

Min, M., Lee, W.S., Kim, Y.H., Bucklin, R.A., 2006. Nondestructive detection of nitrogen in Chinese cabbage leaves using VIS–NIR spectroscopy. HortScience 41 (1), 162–166.

Mishra, A.R., Karimi, D., Ehsani, R., Albrigo, L.G., 2011. Evaluation of an active optical sensor for detection of Huanglongbing (HLB) disease. Biosyst. Eng. 110 (3), 302–310.

Mishra, A.R., Karimi, D., Ehsani, R., Lee, W.S., 2012. Identification of citrus greening (HLB) using a VIS–NIR spectroscopy technique. Trans. ASABE 55 (2), 711–720.

Okamoto, H., Lee, W.S., 2009. Green citrus detection using hyperspectral imaging. Comput. Electron. Agric. 66 (2), 201–208.

Patil, R., Lee, W.S., Shankar, R., Ehsani, R., 2009. Detection and elimination of trash using machine vision and extended de-stemmer for a citrus canopy shake and catch harvester. ASABE Paper No. FL09-129. St. Joseph, Mich., ASABE.

Pourreza, A., Lee, W.S., Raveh, E., Ehsani, R., Etxeberria, E., 2014. Citrus Huanglongbing detection using narrow band imaging and polarized illumination. Trans. ASABE 57 (1), 259–272.

Pydipati, R., Burks, T.F., Lee, W.S., 2006. Identification of citrus disease using color texture features and discriminant analysis. Comput. Electron. Agric. 52 (1), 49–59.

Sankaran, S., Ehsani, R., 2011. Visible-near infrared spectroscopy based citrus greening detection: evaluation of spectral feature extraction techniques. Crop Prot. 30 (11), 1508–1513.

Sankaran, S., Ehsani, R., 2013. Comparison of visible-near infrared and mid-infrared spectroscopy for classification of Huanglongbing and citrus canker infected leaves. Agric. Eng. Int.: CIGR J. 15 (3), 75–79.

Sankaran, S., Ehsani, R., 2012. Detection of Huanglongbing disease in citrus using fluorescence spectroscopy. Trans. ASABE 55 (1), 313–320.

Sankaran, S., Maja, J.M., Buchanon, S., Ehsani, R., 2013. Huanglongbing (citrus greening) detection using visible-near infrared and thermal imaging techniques. Sensors 13, 2117–2130.

Sankaran, S., Ehsani, R., Inch, S.A., Ploetz, R.C., 2012. Evaluation of visible-near infrared reflectance spectra of avocado leaves as a non-destructive sensing tool for detection of laurel wilt. Plant Dis. 96 (11), 1683–1689.

Sengupta, S., Lee, W.S., 2014. Identification and determination of the number of immature green citrus fruit under different ambient light conditions. Biosyst. Eng. 117, 51–61. http://dx.doi.org/10.1016/j.biosystemseng.2013.07.007.

Shin, J., Lee, W.S., Ehsani, R., 2012. Postharvest citrus mass and size estimation using logistic classification model and watershed algorithm. Biosyst. Eng. 113 (1), 42–53.

Yang, C., Lee, W.S., Williamson, J.G., 2012. Classification of blueberry fruit and leaves based on spectral signatures. Biosyst. Eng. 113 (4), 351–362.

Zaman, Q., Schumann, A.W., 2005. Performance of an ultrasonic tree volume measurement system in commercial citrus groves. Precis. Agric. 6 (5), 467–480.

Zaman, Q., Schumann, A.W., Hostler, K.H., 2006. Estimation of citrus fruit yield using ultrasonically-sensed tree size. Appl. Eng. Agric. 22 (1), 39–44.